An accurate Evaluation of Steady State Hydrodynamic Performance of 3D Fin using computational fluid dynamics.

Zulfiqar Nazir [1] and Su Yumin [2]

[1] College of Shipbuilding Engineering, Harbin Engineering University, Nantong Street, Harbin, China, 150001
E-mail: zulfiqar_1981@yahoo.com

[2] College of Shipbuilding Engineering, Harbin Engineering University, Nantong Street, Harbin, China, 150001
E-mail: Suyumin@hrbeu.edu.cn

Abstract

The underwater locomotion and propulsion have provided a stage for the development and application of control methods for designing, optimization and subsequent evaluation of hydrodynamic performance of rudders and control surfaces associated with such underwater vehicles. The study of 3D fin surfaces of an underwater vehicle is an interesting and challenging research subject in the field of underwater locomotion and propulsion for underwater vehicle. In the present study, a computational fluid dynamic (CFD) RANSE simulation of a 3D fin body has been developed to investigate the steady state hydrodynamic coefficients (lift, drag and moment) of 3D fin in interaction with viscous flow by adopting two different grid systems namely structured and unstructured grid, along with detailed discussions on various factors affecting the simulation results using both grid systems. In this study, an implicit pressure-based finite volume method is used for time dependent accurate computation of incompressible flow using second order accurate convective flux discretisation schemes. The present work comprises of two parts, the first part briefly investigates the unstructured grid model and second parts covers in detail the structured grid model and finally both the simulated results are validated against the experimental data along with discussions.

Keywords: 3D Fin, CFD, RANSE, Hydrodynamic Coefficients, Steady State.

Introduction

The development of autonomous underwater vehicles has progressed quite significantly in the past decade due in large part to the increasing interest in unmanned underwater surveillance and monitoring. The study of underwater locomotion has long been a subject of interest to the biological community [1–6]. A large portion of the work that has been performed relevant to swimming vehicles has focused on the task of forward locomotion [7–13]. The stability and maneuvering of underwater vehicle either propelled or autonomous is directly related to the fin and control surfaces of the underwater vehicle, which are the fundamentals of dynamics and control of underwater vehicle. In the past a lot of work has been carried out for the optimization [14] and designing of 3D Fin from 2D foil shapes [15] and very little quantitative research is available on the evaluation of hydrodynamic coefficients of 3D fins in a viscous flow. The two most important hydrodynamic quantities affecting the performance of underwater vehicle are lift and drag associated with the fin surfaces of such underwater vehicle. Almost all the hydrodynamic analyses have attempted to maximize the lift for a given amount of drag, or conversely to minimize the drag for a given amount of lift. The analysis of these quantities for various fin configurations of underwater vehicles forms the basis of most hydrodynamic research. Because of this, reliable methods to compute these forces from available experimental or computational data are essential. Traditionally, hydrodynamic forces have been measured in towing tanks using strain-gauges. This approach is very good for measuring the lift, but the drag of a typical fin surfaces at reasonable angles of incidence is often an order of magnitude less than the lift, and therefore, more difficult to measure. In particular, the presence of the model support makes accurate drag measurement very difficult using this approach. The present paper presents the details of the study of the hydrodynamic performance of a 3D Fin in a steady viscous flow. The families of airfoils known as the NACA 4-series [16] were developed in 1933, improvements to the 4-series later produced the 6-series [16–17] which are the standard 2D surfaces being used at present for the construction of 3D lifting objects, such as hydroplanes, propellers and rudders. Regardless of the type of a lifting surface, its hydrodynamic characteristics will be strongly affected by the shape of the fin section [17]. A convenient way of describing the hydrodynamic characteristics of a fin is to plot the values of the hydrodynamic coefficients against the angle of attack. A measure of the efficiency of the fin as a lifting surface is given by the lift–drag ratio. This ratio increases from zero at zero lift to a maximum value at a moderate lift coefficient, after which it decreases relatively slowly as the angle of attack is further increased. It is desirable for the fin to have the smallest possible drag and maximum lift coefficient for high and moderate speed. Keeping in mind all the above factors experimental model was designed and constructed using the NACA 0018 foil surface with the surface area of 0.16m, ϑ = 10 Degrees, spanwise distance L = 400 mm as shown in Table 1 (All the chordwise distances are in mm). A Series of experiments [18] were conducted at the towing tank facility of HEU for the evaluation of hydrodynamic coefficients of 3D fin for the steady and unsteady state conditions with Reynolds number 8.75×10^5 , dynamic viscosity 0.001003 $kg/m.sec$ and density 998.2 kg/m^3, which are used in the present work for comparison with the simulation results.

br	bt	bc	Lo/br	Lc/bc	bt/br
493.8	306.2	400	0.267	0.224	0.62

Table 1: Parameters of Experimental model.

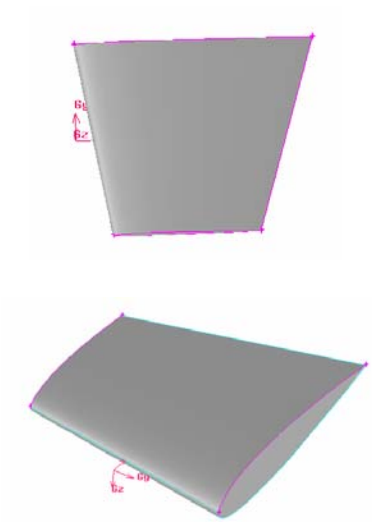

Figure 1: 3D Fin Designed Model.

1. Steady State Analyses

Computational fluid dynamics (CFD) has been constantly developed over the past few decades and now both commercial and in-house codes can provide more robust and accurate results. Combined with the towing tank and wind tunnel test data, CFD can be used in the design process to drive geometry change instead of being used as mainly the design validation tool. The steady state analysis of the fin is simulated by adopting two different grid systems namely the structured and unstructured grid. The accurate prediction of the hydrodynamic coefficients and the flow field around the fin body largely depends upon three factors, namely the control volume domain in which the fin is being simulated, secondly the meshing of the fin which in most of the cases is a greater contributor, and thirdly the physical properties of the fluid interacting with the fin body, here the "physical properties" not only mean the boundary conditions but also includes the various factors such as linearization, discretization and turbulent factors associated with the fluent solver used for the simulation of the steady state flow passing the fin body.

2. Meshing

In order to evaluate the steady state hydrodynamic performance of 3D fin two different types of grid are generated, namely structured and unstructured. Unstructured grid is generated by using the size function with fin as the source for meshing and volume as the attached entity. Tetrahedral cells are used as the basic grid elements placed in irregular fashion around the fin body as shown in fig 2. Here fixed type of size function is generated by taking complete fin body as the source for meshing the entire control volume domain as an attachment. With this particular scheme of meshing cluster of tetrahedral grid elements are generated around the fin body which is the object of interest for evaluation of hydrodynamic performance.

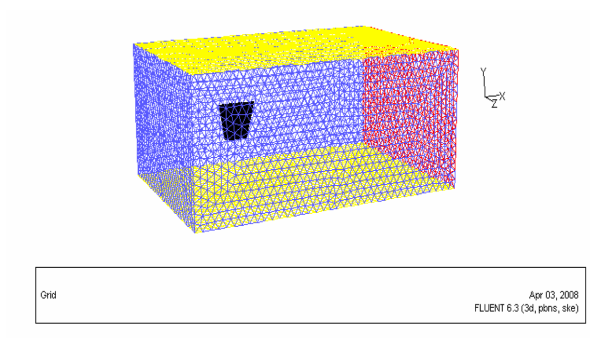

Figure 2: Unstructured Grid Mesh Model.

The purpose of structured mesh is to observe the quantitative change in the magnitude of hydrodynamic coefficients for values of attack angle as compared to the results of unstructured mesh which is narrated later under the heading of results and discussions. Various models were designed and evaluated with changes in the dimensions of the control volume and the flow field bifurcation. Finally two models were found to be having good agreement with the experimental results. Both models have the same dimensions of the control volume and the same number of mesh elements. The fin whose hydrodynamics performance is to be evaluated is divided into six parts in model 1 and eight parts in model 2 as shown in Fig 3 and 4.

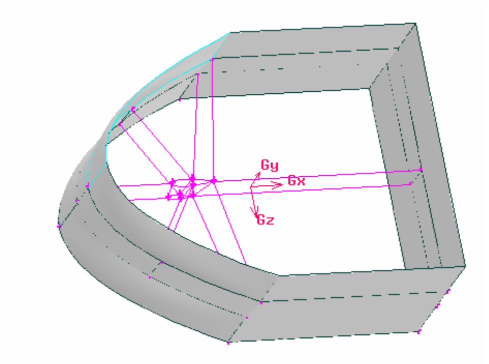

Figure 3: Structured Grid Designed Model 1.

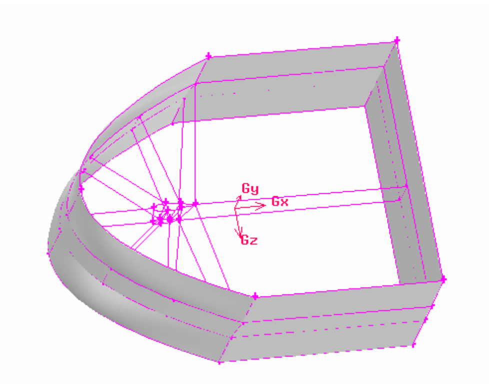

Figure 4: Structured Grid Designed Model 2.

The inflow velocity is taken along the x-axis and inlet is designed with the wider curve so that more elements can be generated on the upper and lower foil surfaces of the fin which will contribute in the effective multiblock C-type structured grid generation. The inverted edge ratio is used for all the edges joining at the fin surface in such way so that maximum numbers of elements are placed near the fin surface. The edges which are joining the lower and upper fin surface are meshed using bell shaped element ratio creating more quadrilateral panels at the corners of upper and lower foil surface.

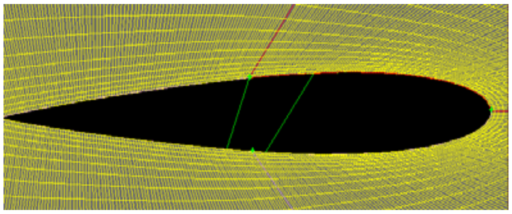

Figure 5 View of Quadrilateral Panels Around Foil Surface.

The other important factor which is considered in the meshing of the edges is the same interval size for the multipoint edges that is the point on the fin surface where two or more edges are sharing common vertex. By doing so the quadrilateral panels near the fin surface are of equal size so that the flow is well aligned with the generated grid.

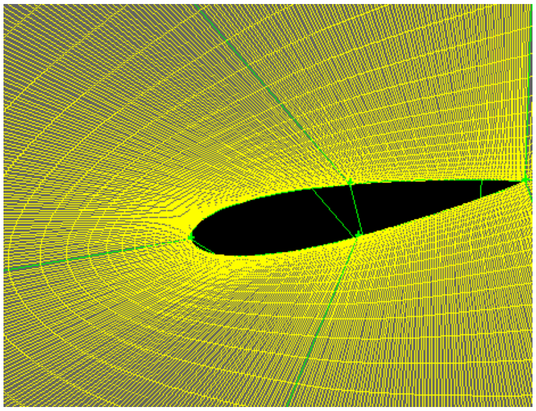

Figure 6 View Of Mesh Upper Foil Surface.

3. Turbulent Model and Boundary Conditions

This simulation is aimed to predict the hydrodynamic performance of 3D fins placed in a viscous flow. The K- ε turbulence model is implemented in the simulation, which is often described to be the “workhorse” of practical engineering flow calculations. The standard K-ε turbulence model with the standard wall functions is selected, and the pressure based RANSE solver with the implicit formulation the default option of the solver is used for solving the turbulent model. The K-ε turbulent model is robust, economic and reasonably accurate enough for a wide range of turbulent flows. For the initial simulations the standard K- ε turbulence model, with the default standard settings was found to be sufficiently accurate. In order to define Boundary conditions, the top and bottom surfaces of the control volume are taken as the symmetric and the fin body is defined as a wall with a roughness constant 0.5. The outlet is defined as outflow with flow rate weighing equal to one. Three faces of the control volume are taken as the velocity inlet and the method for specifying the inflow velocity is chosen as the velocity component method with the magnitude of velocity 2.198 m/s. The x and z components of the inflow velocity are defined by using the experimental values of attack angle at which the experimental model was tested for evaluation of hydrodynamic performance.

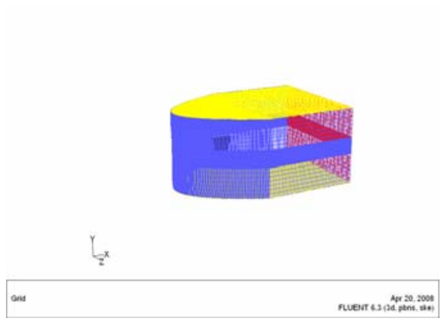

Figure 7 Structured Grid Mesh Model and Boundary Conditions.

4. Results and Discussions

Once the solution is converged as per the standard FLUENT time independent convergence criteria [19] simulation is further set up for the evaluation of hydrodynamic coefficients. Lift coefficient is defined as along the z-axis and drag coefficient along the x-axis. Moment coefficient is calculated about the y axis. The moment coefficient about this axis also termed as pivot axis, will be the same at all the points lying on the axis. The coordinates of these points are the moment centre coordinates (X = -0.918, Y = 0, 0.1, 0.2, 0.3,-0.1,-0.2, Z = 0), used for the calculation of moment coefficient, x and z coordinates are fixed only y coordinate has variable magnitude. The results of hydrodynamic coefficients are plotted against the values of attack angle varying from zero to thirty one degrees as summarized in Fig 9-14. Statistical simulation data reveals that for small values of attack angle simulation results show very small difference when compared with the experimental data. However with the increase in the attack angle the percentage of difference also increases until it levels of near the stall point [16] at 31.678 degrees. The lift coefficient is observed to have 15% difference from experimental in case of unstructured grid and that of 9.3% in case of structured grid, which is noticeably smaller than the unstructured grid lift coefficient. However for the same value of attack angle the drag coefficient is found to have a difference of 33.76% for structured and 15.89% for unstructured grid and the moment coefficient which is calculated about the y-axis is having 30% difference for structured and 20.46% for unstructured as compare to the experimental data. The results of structured grid simulation have shown improvement in case of lift coefficient but along with the increase in drag coefficient, comparatively there is very little difference in results of structured and unstructured grid except for the C_L / C_D slope as shown in Fig 15 in which the results of unstructured grid simulation are in close agreement with the experimental, however in the case of structured grid simulation due to enhanced drag coefficient the C_L / C_D slope is not so close to that of experimental data, especially for an initial attack angle of 3.8191 it is only 21% of the experimental C_L / C_D , however with the increase in the attack angle it is found to be in close agreement with that of experimental data. In general the results of the two grid methods are in close agreement with each other. This is understandable considering CFD simulations for both grid methods are very similar in control volume domain, turbulent model, solver formulation and the boundary conditions. There are various advantages [20] in a structured grid one of which being the flow well aligned with the grid due to default option of quadrilateral/hexahedral cells. Which may also contributed to the differences in the hydrodynamic coefficients (lift, drag and moment coefficient).

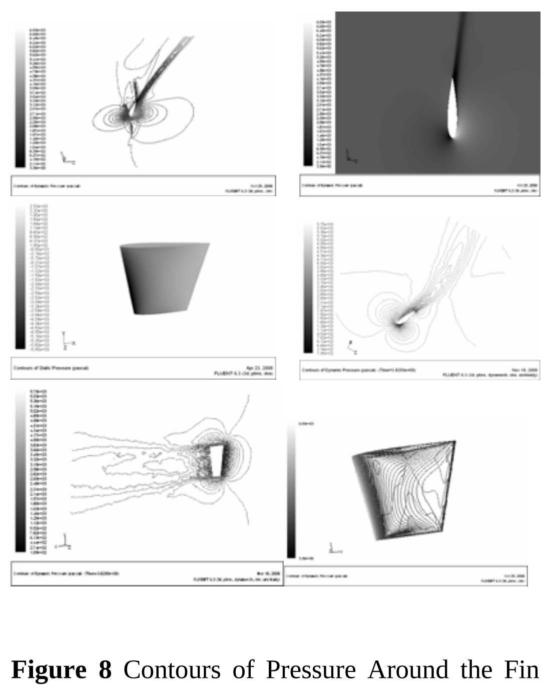

Figure 8 Contours of Pressure Around the Fin body.

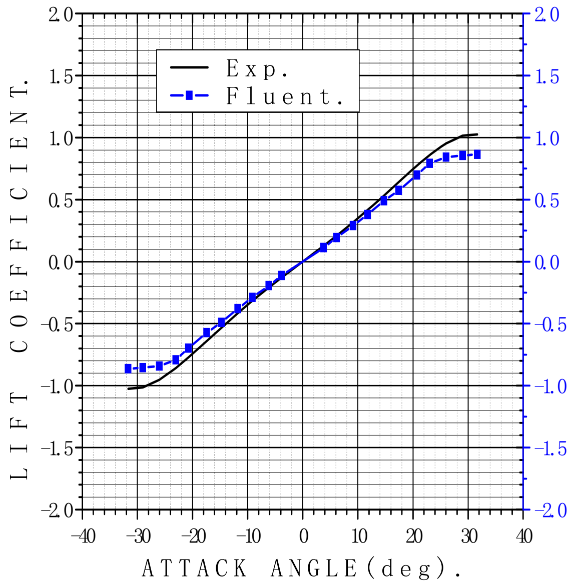

Figure 9 Steady State Unstructured Grid Lift Coefficient.

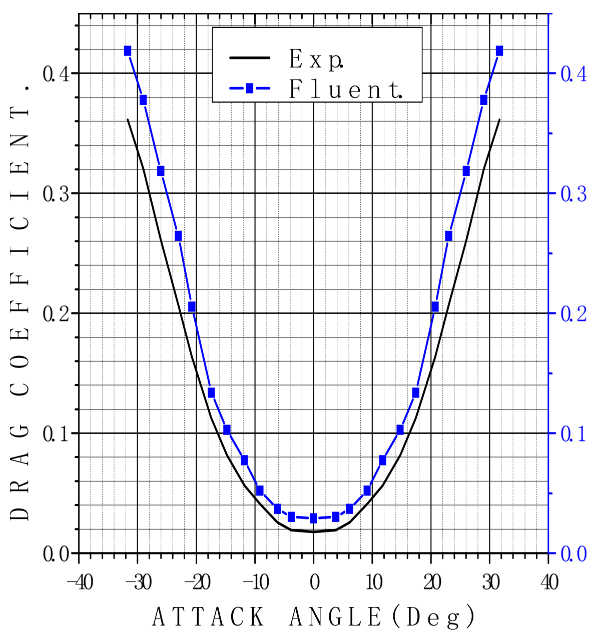

Figure 10 Steady State Unstructured Grid Drag Coefficient.

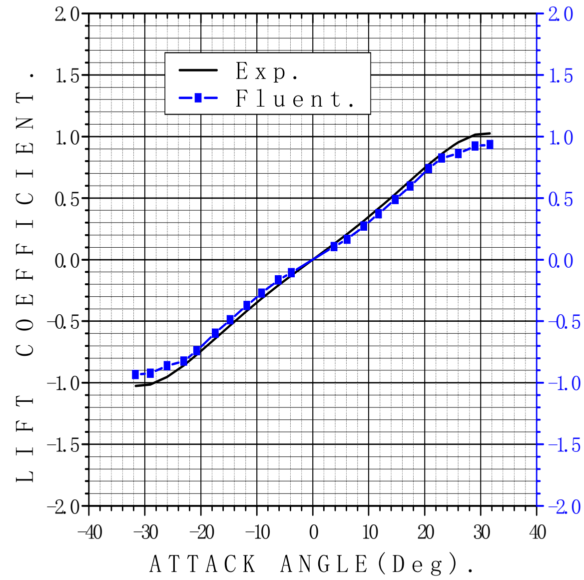

Figure 11 Steady State Structured Grid Lift Coefficient.

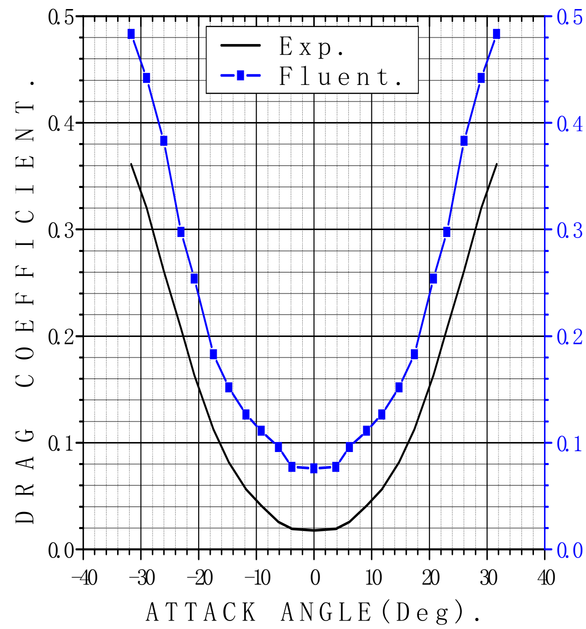

Figure 12 Steady State Structured Grid Drag Coefficient.

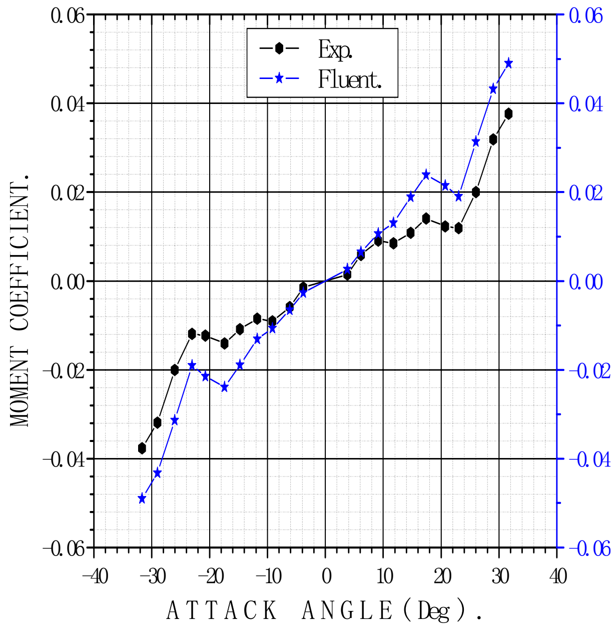

Figure 13 Steady State Structured Grid Moment Coefficient.

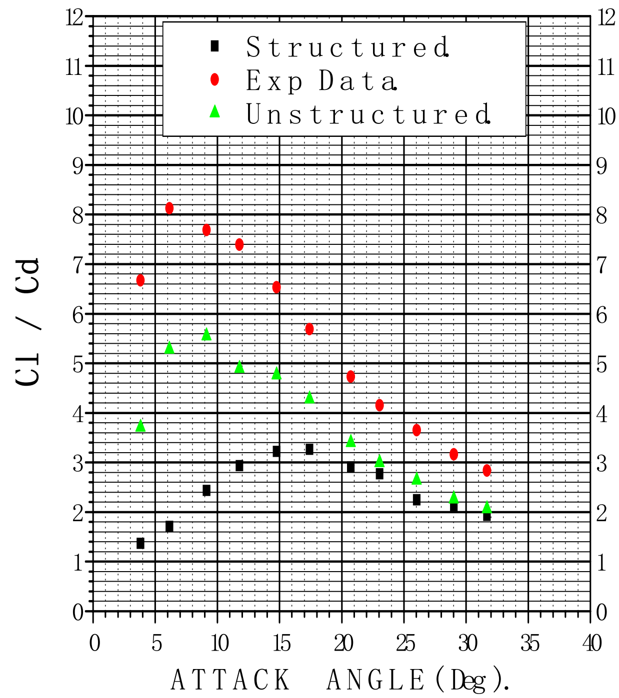

Figure 15 Lift–Drag Ratios C_L / C_D.

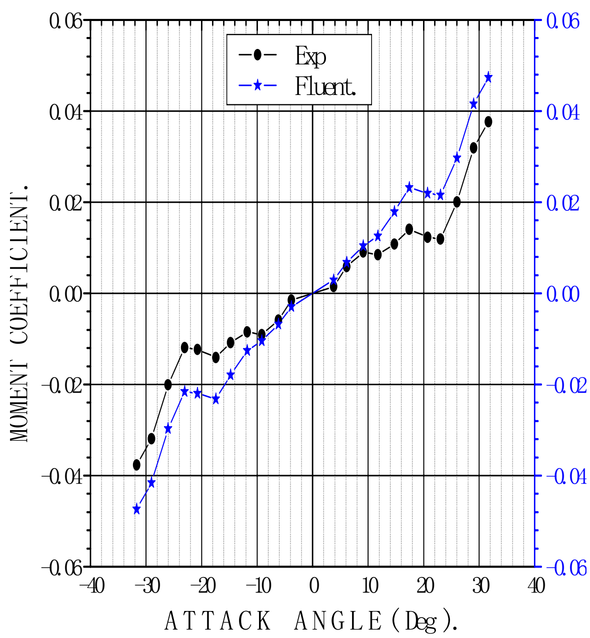

Figure 14 Steady State Unstructured Grid Moment Coefficient.

5. Conclusion

The work in this paper has addressed the evaluation of steady state hydrodynamic coefficients of 3D fin in a viscous flow. A steady state analysis is simulated by adopting two different grid systems, namely structured and unstructured grids. The results of both simulations are found in close agreement with the experiment, hence validating the present work as an effective representation of evaluation of steady state hydrodynamic coefficients of 3D fins which can be further extended for analyses of stability and maneuvering of fin actuated underwater vehicles.

References

[1] S. Childress, Mechanics of swimming and flying. Cambridge: Cambridge University Press, 1981.

[2] J. Lighthill, Mathematical Bio fluid dynamics. Philadelphia: SIAM, 1975.

[3] J. Newman and T. Wu, Hydrodynamical aspects of fish swimming," in Swimming and Flying in Nature, Vol 2. T. Wu, C. Brokaw, and C. Brennen, Eds. New York: Plenum Press, 1975, pp. 615–34.

[4] D. Weihs, "A hydrodynamical analysis of fish turning maneuvers," Proc. R. Soc. Lond. B, vol. 182, pp. 59–72, 1972.

[5] I. Spierts and J. van Leeuwen, "Kinematics and muscle dynamics of C- and S-starts of carp (cyprinus carpio L.)," J. Exp. Biology, vol. 202, pp 393–406, 1999.

[6] P. Domenici and R. Blake, "The kinematics and performance of fish fast-start swimming," J. Exp. Biology, vol. 200, pp. 1165–1178, 1997.

[7] D. Barrett, M. Grosenbaugh, and M. Triantafyllou, "The optimal control of a flexible hull robotic undersea vehicle propelled by an oscillating foil" in Proc. 1996 Symp. Aut. Underwater Veh. Tech., 1996, pp. 1– 9.

[8] K. Morgansen, V. Duindam, R. Mason, J. Burdick, and R. Murray, "Nonlinear control methods for planar carangiform robot fish locomotion," in Proc. IEEE Int. Conf. Rob. Aut. 2001.

[9] P. Vela, K. Morgansen, and J. Burdick, "Second order averaging methods for oscillatory control of under actuated mechanical systems," 2002, to appear in Proceedings of the 2002 American Control Conference.

[10] S. Saimek and P. Li, "Motion planning and control of a swimming Machine," in Proc. Amer. Contr. Conf., 2001, pp. 125–30.

[11] R. Mason and J. Burdick, "Propulsion and control of deformable bodies in an ideal fluid," in Proc. IEEE Int. Conf. Rob. Aut. 1999, pp. 773–80.

[12] S. Kelly, R. Mason, C. Anhalt, R. Murray, and J. Burdick, "Modeling and experimental investigation of carangiform locomotion for control," in Proc. Amer. Contr. Conf., 1998, pp. 1271–6.

[13] J. Liu, I. Dukes, R. Knight, and H. Hu, "Development of fish-like swimming behaviors for an autonomous robotic fish," in Proceedings of the Control'04. University of Bath, England: IEE, September 2004, ID217.

[14] Wenbin Song, Andy Keane, Hakki Eres, Graeme Pound, and Simon Cox "Two Dimensional Airfoil optimization Using CFD in a Grid Computing Environment" School of Engineering Sciences University of Southampton Highfield, Southampton, SO17 1BJ, UK.

[15] Dave Carswell and Nick Lavery " 3D solid fin model construction from 2D shapes using non-uniform rational B-spline surfaces " Materials Research Centre, University of Wales Swansea, Singleton Park, Swansea SA2 8PP, United Kingdom.

[16] Abbott IH, Doenhoff AEv, Stivers LS. Summary of airfoil data, National Advisory Committee for Aeronautics 824, 1945.

[17] Jacobs EN. Preliminary report on laminar-flow airfoils and new methods adopted for airfoil and boundary-layer investigations, NACA WR L-345, 1939.

[18] Tong Zhen-Ming, Zhao Xiao-dong, and Ding Yong. Series experiments of steady and unsteady 3D hydrofoil, research report of HEU 2004.

[19] Fluent Tutorials.

[20] Gambit Tutorials meshing and grid literature Fluent Tutorials.